Variation Analysis of Root System Development in Wheat Seedlings Using Root Phenotyping System

Ekundayo Adeleke [1], Reneth Millas [1], Waymon McNeal [1], Justin Faris [2] and Ali Taheri [1,*]

[1] Department of Agricultural and Environmental Sciences, Tennessee State University, Nashville, TN 37209, USA; eadeleke@Tnstate.edu (E.A.); renz_millas@yahoo.com (R.M.); waymon.mcneal28@gmail.com (W.M.)

[2] USDA-ARS Cereal Crops Research Unit, Edward T. Schafer Agricultural Research Center, 1616 Albrecht BLVD N., Fargo, ND 58102, USA; Justin.Faris@ars.usda.gov

* Correspondence: ataheri1@tnstate.edu or atahery@gmail.com; Tel.: +1-(615)-963-6056

Abstract: Root system architecture is a vital part of the plant that has been shown to vary between species and within species based on response to genotypic and/or environmental influences. The root traits of wheat seedlings are critical for their establishment in soil and evidently linked to plant height and seed yield. However, plant breeders have not efficiently developed the role of RSA in wheat selection due to the difficulty of studying root traits. We set up a root phenotyping platform to characterize RSA in 34 wheat accessions. The phenotyping pipeline consists of the germination paper-based moisture replacement system, image capture units, and root-image processing software. The 34 accessions from two different wheat ploidy levels (hexaploids and tetraploids), were characterized in ten replicates. A total of 19 root traits were quantified from the root architecture generated. This pipeline allowed for rapid screening of 340 wheat seedlings within 10 days. At least one line from each ploidy (6× and 4×) showed significant differences ($p < 0.05$) in measured traits, except for mean seminal count. Our result also showed a strong correlation (0.8) between total root length, maximum depth and convex hull area. This phenotyping pipeline has the advantage and capacity to increase screening potential at early stages of plant development, leading to the characterization of wheat seedling traits that can be further examined using QTL analysis in populations generated from the examined accessions.

Keywords: root system architecture; high-throughput phenotyping; root traits; *Triticum* sp.; germination paper-based system

1. Introduction

Roots serve as boundaries between plants and complex soil mediums. Aside from anchoring the plant to soil medium [1], another major function of the root is to provide plant access to nutrient and water uptake. Roots are also essential for forming symbioses with beneficial microbes in the rhizosphere and used as storage organs [1,2]. Therefore, roots are critical in the maintenance of plant health. Many environmental factors interact with soils, leading to the spatial and temporal heterogenous nature of the soil [3]. This spatial heterogeneity makes studying the roots in soil a multifaceted challenge. The spatial distribution of roots in soil under field conditions demonstrates a considerable amount of variability, since roots respond to heterogeneity in the soil and environmental cues allowing plants to overcome challenges posed by biotic or abiotic factors in soil environment [2]. This spatial distribution of the root system in soil is referred to as root system architecture (RSA). RSA usually describes the morphological and structural organization of the root [4]. RSA is important for plant productivity because it determines the plant's ability to successfully access major heterogenous edaphic resources [5]. Therefore, RSA has a direct influence on grain yield.

Wheat is a major cereal crop of global importance. It is grown in temperate zones and has remained a worldwide staple food [6]. It belongs to the *Triticum* genus, which includes species such as *T. aestivum* ssp. *aestivum* L. (common wheat, $2n = 6x = 42$, AABBDD genomes), an allohexaploid and the most cultivated wheat species in the world, accounting for 95% of global wheat production [7]; *T. turgidum* ssp. *durum* (Desf.) Husnot (durum wheat, $2n = 4x = 28$, AABB genomes), a tetraploid that is the second most cultivated wheat species accounting for 5%-8% of global wheat production [8]; and *T. turgidum* ssp. *dicoccum* (Schrank) Schübl (cultivated emmer wheat, $2n = 4x = 28$, AABB genomes) a tetraploid that is one of the earliest crops domesticated in the Near East [9]. So far, most wheat breeding programs have focused on aboveground phenotypic traits while ignoring the belowground traits. Although it is easier for breeders to consider aboveground traits because they are the most visible to the eye, belowground traits should not be ignored because they play equally important roles in plant productivity [1,2].

In cereal grains, the radicle emerges first and is covered with a protective sheath called the coleorhiza [10,11]. After the roots have extended somewhat further, the coleoptile emerges and grows rapidly. The seedling will then possess a unique RSA [12] by the time they are at the germination stage (Figure 1), and this has a major impact on the early establishment of the seedling and its productivity at later growth stages.
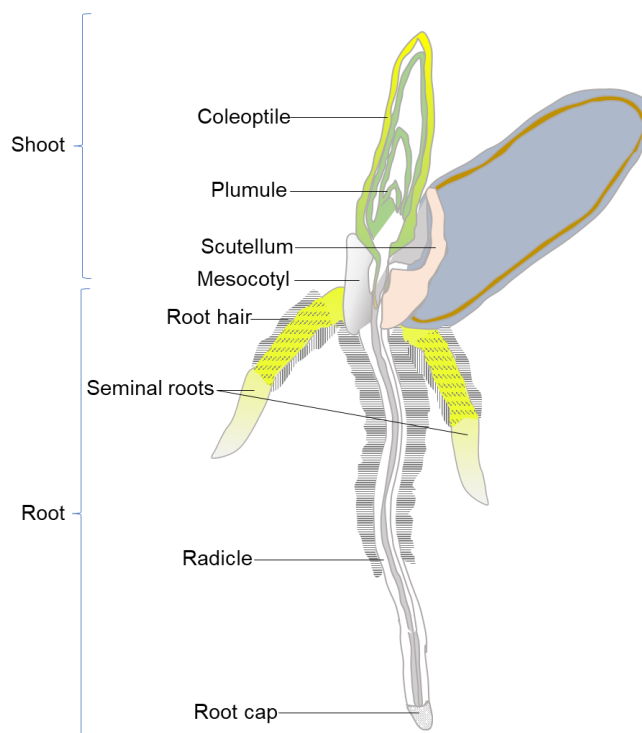

Figure 1. Annotated diagram of germinating 4 day old wheat grain. The kernel is showing root development that includes root cap, radicle, seminal roots, and root hairs; and shoot development that includes mesocotyl, plumule, and coleoptile at Zadok's growth stage 07 [13].

For wheat to grow and produce enough yield, it is important to understand and select unique traits in RSA as well, using aboveground traits. Abiotic stresses due to climate change have affected wheat productivity by limiting the uptake of nutrients and water [5]. This is one reason that progress in obtaining wheat varieties with increased yields has been hindered [14,15]. One way to alleviate the adverse effects of these factors on wheat yield is to select unique traits and manipulate the underlying genes associated with wheat RSA so as to optimize the water and nutrient uptake. Although root phenotyping is critical for optimizing RSA in crops, the study of roots in the field is still in its infancy. The traditional techniques used for studying roots in the field including soil coring, trenching, or

shovelomics [16,17]. Most of these techniques involve the excavation of the roots, washing off the soil on a sieve and afterward quantifying the root traits. These methods are time consuming, labor intensive, low-throughput and not efficient for genetic studies. In recent years, the use of soil-less media, hydroponics, semi-hydroponics or gel-based media have been used to study root development [18,19]. Current advancements in software development for imaging, automation, and robotics have increased the possibility of high-throughput, non-invasive studies of roots [20]. The germination paper-based approach (growth pouch) has been used to measure axile and lateral roots (Figure 2B) of maize [21] and has been recently modified for high-throughput measurement in rapeseed, barley [22], and common bean [23]. The germination paper-based approach developed by Hund et al. [21] required a plastic covering that stuck to the root and required intervention to remove the covering [24]. Although modified forms of this growth pouch have been reported [12,24–26], there is still a knowledge gap yet to be filled in the development of root phenotyping systems and high-throughput screenings of wheat. The wheat accessions selected for this study have never been reported for root variation analysis to the best of our knowledge. They are unique and represent a diverse pool of collection from different origins representing five continents (North America, South America, Europe, Africa, and Asia) (Table 1).
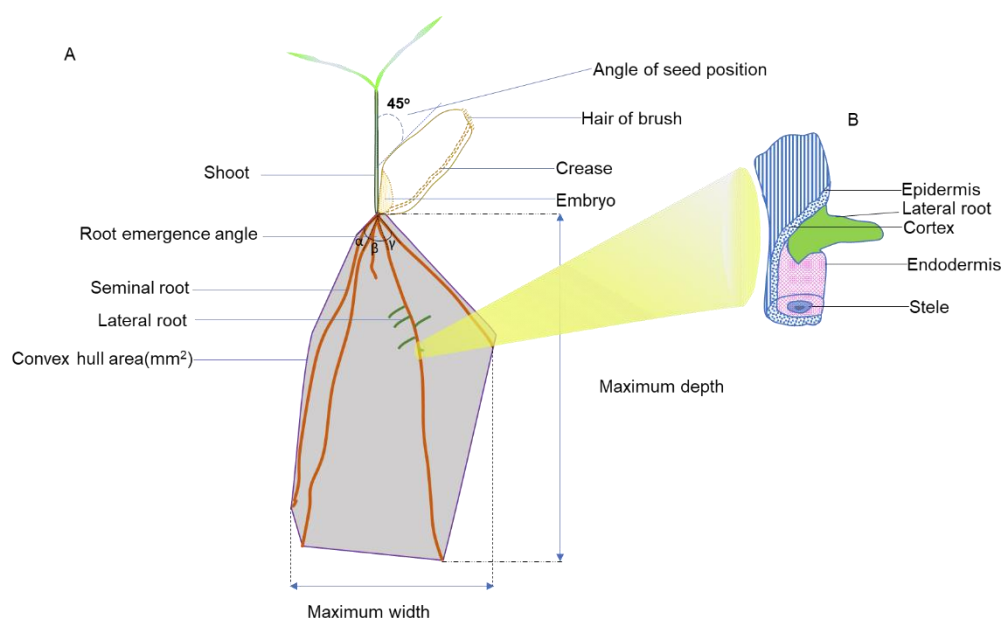

Figure 2. (**A**) Summary of seedling features within the growth system and the positioning of the seed. The positioning of the seed at 45° to the vertical plane of the growth system permitted the precise upward development of the coleoptile and concomitant downward growth of the roots. The crease of the seed is inverted to face the horizontal plane of the pouch, allowing the roots to grow away from the germination paper. (**B**) Illustration of lateral root emerging from the overlying tissues of the primary seminal root.

High-throughput screening can expedite the selection of novel traits for crop improvement in plant breeding [15]. However, high-throughput screening of root traits is often limited by the lack of suitable phenotyping growth systems [27]. Therefore, the main objective of this study was to evaluate variation in the RSA of seedlings from 34 wheat accessions for different root traits using a high-throughput root phenotyping pipeline.

2. Materials and Methods

Phenotyping of the 34 wheat accessions was divided into three stages, first, setting up the experiment on the platform; second, the acquisition of RSA images; and third, the analysis of acquired images using open source software (RootNav) [28] (Figure 3).
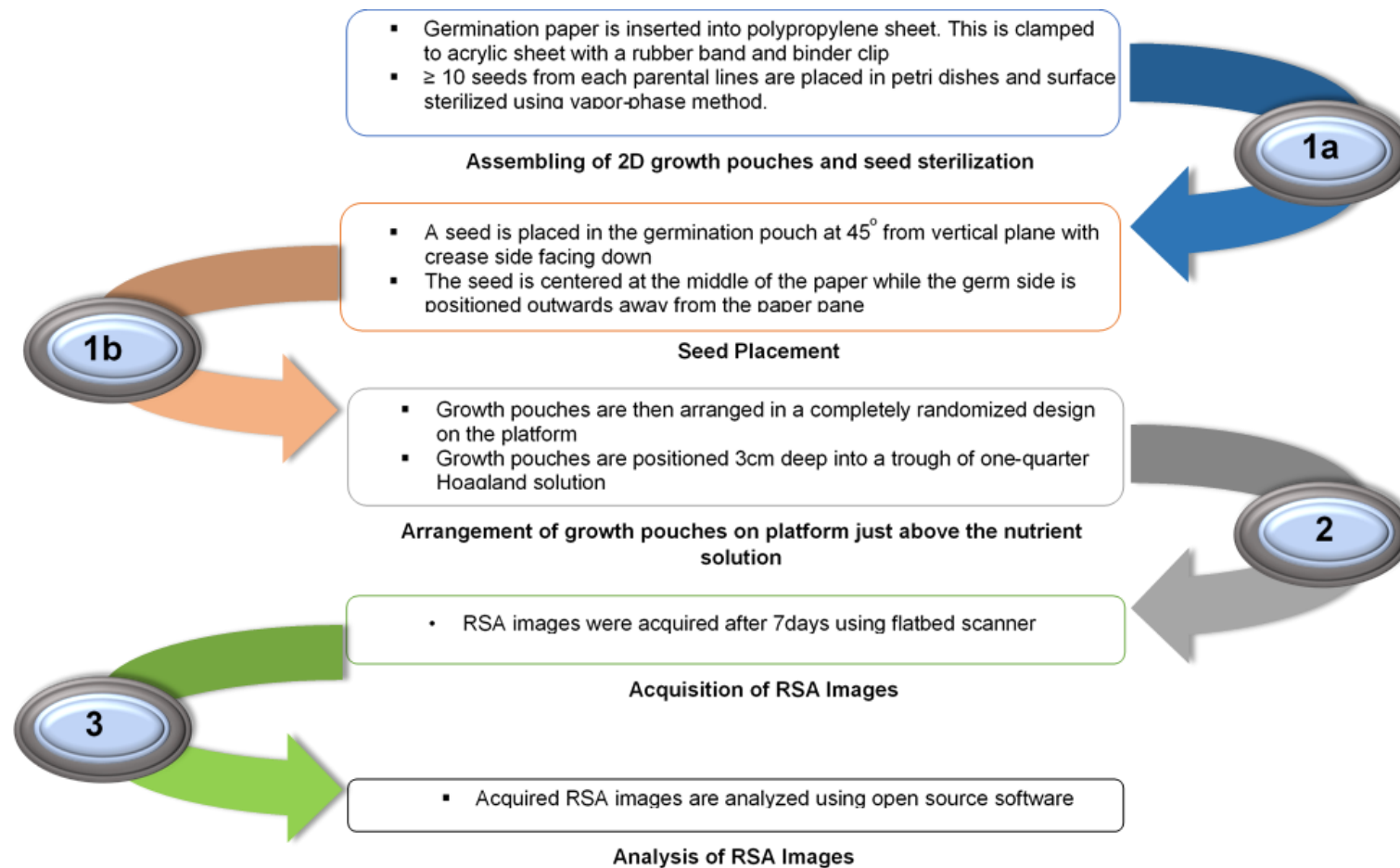
- Germination paper is inserted into polypropylene sheet. This is clamped to acrylic sheet with a rubber band and binder clip
- ≥ 10 seeds from each parental lines are placed in petri dishes and surface sterilized using vapor-phase method.

Assembling of 2D growth pouches and seed sterilization

1a

- A seed is placed in the germination pouch at 45° from vertical plane with crease side facing down
- The seed is centered at the middle of the paper while the germ side is positioned outwards away from the paper pane

Seed Placement

1b

- Growth pouches are then arranged in a completely randomized design on the platform
- Growth pouches are positioned 3cm deep into a trough of one-quarter Hoagland solution

Arrangement of growth pouches on platform just above the nutrient solution

2

- RSA images were acquired after 7days using flatbed scanner

Acquisition of RSA Images

3

- Acquired RSA images are analyzed using open source software

Analysis of RSA Images

Figure 3. Schematic illustrating the three major steps of the root phenotyping pipeline. The first step is seed sterilization and the assembling of 2D growth pouches (1a), and the placement of seeds in respective pouches accordingly and placement into the tanks (1b). The second step involves the acquisition of RSA images using a flatbed scanner (2). The third step is the analyses of RSA images acquired in the second step (3).

The 34 accessions from different wheat species were obtained from a USDA-ARS cereal crop research unit (Fargo, ND, USA) and divided into two separate groups based on their ploidy level (hexaploid vs. tetraploid) (Table 1). The hexaploid category was made up of common wheat, spelt wheat and synthetic hexaploid wheat (SHW). SHW is hexaploid wheat that is created artificially by the introduction of additional genetic resources from tetraploid and diploid relatives to develop wheat with a broader genetic basis. SHW lines are quite useful in introducing agronomically needed traits into common wheat from wild genetic relatives [29]. In this experiment, SHW lines were selected for root phenotyping with the accession Largo selected as the reference accession based on SHW biomass uniqueness and density [29]. The tetraploid group of accessions consisted of durum (*T. turgidum* ssp. *durum*), Persian (*T. turgidum* ssp. *carthlicum*), cultivated emmer (*T. turgidum* ssp. *dicoccum*) and wild emmer (*T. turgidum* ssp. *dicoccoides*) wheat. For the tetraploid group, the durum line Rusty was selected as the reference accession.

Table 1. The common name, taxonomy, origin, and source of 34 different accessions assessed for its seedlings root system architecture (RSA).

Accession	PI/CItr	Common Name	Taxon	Subspecies	Ploidy	Origin
Largo	CItr 17895	Synthetic hexaploid wheat	*Triticum turgidum × Aegiliops tauschii*	Synthetic	6×	U.S., North Dakota
ND495	N/A	Common wheat	*Triticum aestivum*	aestivum	6×	U.S., North Dakota
Grandin	PI 531005	Common wheat	*Triticum aestivum*	aestivum	6×	U.S., North Dakota
BR34	N/A	Common wheat	*Triticum aestivum*	aestivum	6×	Brazil
Chinese Spring	CItr 14108	Common wheat	*Triticum aestivum*	aestivum	6×	China
Arina	N/A	Common wheat	*Triticum aestivum*	aestivum	6×	Switzerland
Forno	N/A	Common wheat	*Triticum aestivum*	aestivum	6×	Switzerland
Sumai 3	PI 481542	Common wheat	*Triticum aestivum*	aestivum	6×	China
Chinese Spring-DIC 5B	N/A	Common wheat	*Triticum aestivum*	aestivum	6×	U.S., Missouri
Bobwhite	PI 520554	Common wheat	*Triticum aestivum*	aestivum	6×	Mexico, CIMMYT
Salamouni	PI 182673	Common wheat	*Triticum aestivum*	aestivum	6×	Lebanon
Katepwa	N/A	Common wheat	*Triticum aestivum*	aestivum	6×	Canada
M3	N/A	Synthetic hexaploid wheat	*Triticum turgidum × Aegiliops tauschii*	Synthetic	6×	Mexico, CIMMYT
PI277	PI 277012	Spelt wheat	*Triticum aestivum*	spelta	6×	Spain
M6	N/A	Synthetic hexaploid wheat	*Triticum turgidum × Aegiliops tauschii*	Synthetic	6×	Mexico, CIMMYT
Kulm	PI 590576	Common wheat	*Triticum aestivum*	aestivum	6×	U.S., North Dakota
Opata85	PI 591776	Common wheat	*Triticum aestivum*	aestivum	6×	Mexico, CIMMYT
TA4152-60	N/A	Synthetic hexaploid wheat	*Triticum turgidum × Aegiliops tauschii*	Synthetic	6×	Mexico, CIMMYT
TA4152-19	N/A	Synthetic hexaploid wheat	*Triticum turgidum × Aegiliops tauschii*	Synthetic	6×	Mexico, CIMMYT
P503	N/A	Spelt wheat	*Triticum aestivum*	spelta	6×	Iran
Divide	N/A	Durum wheat	*Triticum turgidum*	durum	4×	U.S., North Dakota
Rusty	PI 639869	Durum wheat	*Triticum turgidum*	durum	4×	U.S., North Dakota
Ben	N/A	Durum wheat	*Triticum turgidum*	durum	4×	U.S., North Dakota
Lebsock	N/A	Durum wheat	*Triticum turgidum*	durum	4×	U.S., North Dakota
Langdon	N/A	Durum wheat	*Triticum turgidum*	durum	4×	U.S., North Dakota
Altar84	N/A	Durum wheat	*Triticum turgidum*	durum	4×	Mexico, CIMMYT
PI193	PI 193833	Cultivated emmer	*Triticum turgidum*	dicoccum	4×	Ethiopia
PI410	PI 41025	Cultivated emmer	*Triticum turgidum*	dicoccum	4×	Russia
PI947	PI 94749	Persian wheat	*Triticum turgidum*	carthlicum	4×	Georgia
PI481	PI 481521	Wild emmer	*Triticum turgidum*	dicoccoides	4×	Israel
PI478	PI 478742	Wild emmer	*Triticum turgidum*	dicoccoides	4×	Israel
TA106	N/A	Wild emmer	*Triticum turgidum*	dicoccoides	4×	Israel
Israel A	N/A	Wild emmer	*Triticum turgidum*	dicoccoides	4×	Israel
PI272	PI 272527	Cultivated emmer	*Triticum turgidum*	dicoccum	4×	Hungary

2.1. Experimental Design and Seed Treatment

Each accession was planted in ten replicates in a completely randomized design. The seeds were surface sterilized in a chemical hood (Labconco Inc., MO, USA) using the chlorine gas (vapor-phase) method used by Clough and Bent [30]. Ten seeds (or more) were placed in open Petri dishes (previously labeled with chlorine resistant markers) in a 10L desiccator jar. A 3 ml aliquot of 12N HCl was added to a 250 mL beaker containing 100 mL of 8.3% sodium hypochlorite before sealing the desiccator. The seeds remained in the desiccator for 4 h.

2.2. Design of Experimental Platform

A schematic illustration of the stages and flow of the experimental system is presented in Figure 3. We developed a growth pouch system based on the earlier platform designed by Hund et al. [21] for maize. Each sterilized seed was placed into a germination paper pouch, that was constructed from blue germination paper (21.6 × 28 cm; Anchor Paper Company, St Paul, MN, USA) inserted into Staples® standard clear polypropylene sheet protectors (Staples Inc, MA, USA) (Figures 3 and 4A). The bottom edges of these sheet protectors were removed to allow for capillary movement of distilled water and nutrient solution up the germination papers. Two germination pouches were then firmly held to either side of a clear stiff acrylic plate (0.5 × 24 × 30 cm; Acme Plastic Woodland Park, NJ, USA) with a rubber band and a binder clip (Staples Inc, MA, USA) (Figure 4A). The acrylic plates also had extended overhangs (0.5 × 1.5 × 1.0 cm) that fit into a metal support frame that was situated in the top of a customized black polypropylene tank (54.5 × 42.5 × 6.0 cm) (Figure 4C). The 2-D growth systems hung so that they were positioned about 3 cm deep into the liquid media within the tank (Figure 4B). The liquid solution consisted of 12 L of distilled water that was interchanged with modified one-quarter Hoagland's solution [31] three days after germination using a pump. The composition of the nutrient solution was 1.25 mM KNO_3; 0.625 mM KH_2PO_4; 0.5 mM $MgSO_4$; 0.5 mM $Ca(NO_3)_2$; 17.5 μM H_3BO_3; 5.5 μM $MnCl_2$; 0.5 μM $ZnSO_4$; 0.062 μM Na_2MoO_4; 2.5 μM $NaCl_2$; 0.004 μM $CoCl_2$; and 12.5 μM Fe-EDTA. The final pH of the nutrient solution was adjusted to pH 6.2.

A single seed from each accession was placed into a germination paper pouch at 2.5 cm below the top, with the crease-side down, at about a 45° orientation from the vertical plane (Figure 4A). Positioning the seed at this angle provided two main benefits. First, it allowed the phototrophic response of the coleoptile to align with the vertical plane without rerouting its mesocotyl. Second, the position also benefitted the seedling RSA by supporting root emergence away from the germination paper, resulting in easier image acquisition. Each germination pouch containing two seeds (one on each side of the acrylic plate) was arranged on the phenotyping platform in a growth room that was fitted with a growth lamp set at photoperiod of 14 h light and 10 h dark with 400 μmol m^{-2} s^{-1} flux density at 22 °C. After 7 days, with almost all seedlings at growth stage 10 [21], each growth pouch was removed from the platform, the polypropylene sheets were cut open on one side, and a side of each sheet was carefully opened to reveal the blue germination paper.

2.3. Imaging and Analysis

Imaging of the roots was carried out using a Flatbed scanner (HP Inc, Spring, TX, USA). The acquired images were saved as standardized compressed image formats (JPG files), which were then imported as new files into the RootNav software. Each image is then converted to a probability map (inverted images) in the software, with the root images represented as clustered groups of pixels using the gaussian mixture model based on the varying intensities of the pixels [28]. The RootNav allows expectation maximization clustering to assign the best appearance likelihood of the pixels from root images against the background, creating a model that can be fit from the seed point (source) to the root apices.

The RSA images acquired from the wheat seedling were then semi-automatically measured with open source RootNav software [28], and the predefined model setting for wheat seedling was used to acquire measurements of the traits. The root traits that were measured for each replicate included: total

length (TL, is the summation of all the root length—mm), seminal length (the total length of seminal roots—mm), lateral length (the total length of lateral roots—mm), mean seminal length (ASL, is the mean value of the total length of the seminal roots—mm), mean lateral length (mean value of the total length of lateral roots—mm), seminal count (PC, is the number of seminal roots), lateral count (number of lateral roots), mean seminal count (mean value of the total number of seminal roots), mean lateral count (mean value of the total number of lateral roots), average seminal emergence angle (measurement of emergence angle of the seminal roots—degrees), average lateral emergence angle (measurement of emergence angle of the lateral roots—degrees), average seminal tip angle (mean value of the measurement of angle in the seminal root tips—degrees), average lateral tip angle (mean value of the measurement of angle in the lateral root tips—degrees), root tip angle (the measurement of angle in the seminal root tips—degrees), maximum width (MW, is the furthermost width of the root system along horizontal axis—mm), maximum depth (MD, is the furthermost depth of the root system along vertical axis—mm), width–depth ratio (WDR, is the ratio of the maximum width to the maximum depth of the root system), centroid (the coordinates of the center of mass of root system along the horizontal, Cen_X and vertical axes, Cen_Y—mm), convex hull area (CHA, is the area of the smallest convex polygon covering the boundaries of the root system—mm^2), and tortuosity (the average curvature of the seminal roots).
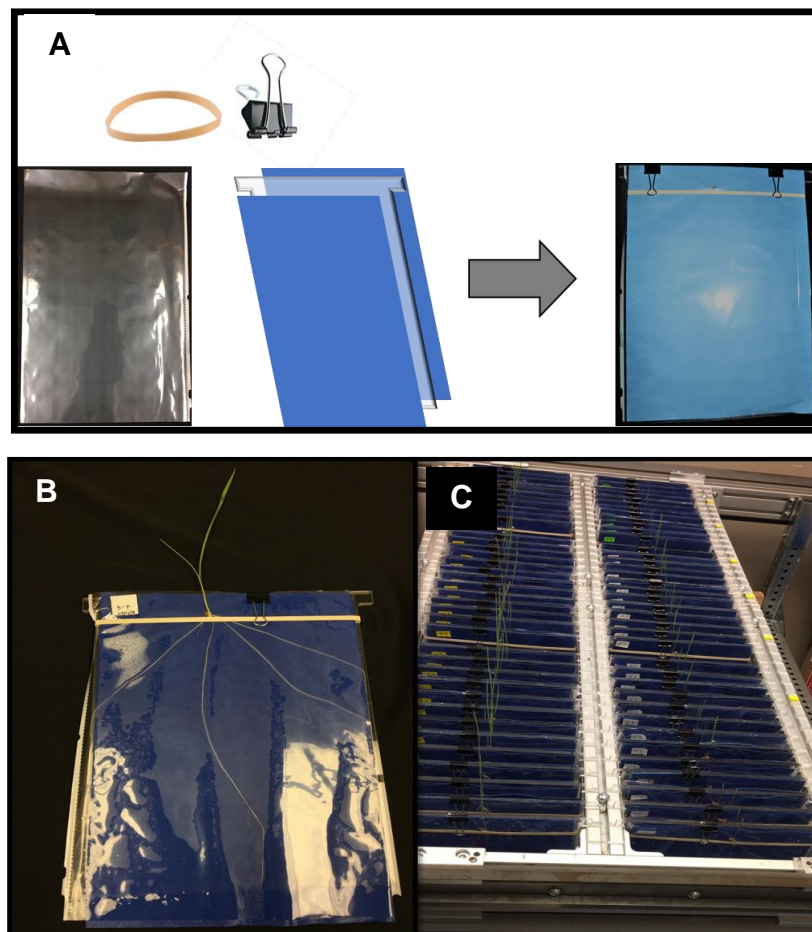

Figure 4. A customized high-throughput seedling root phenotyping platform, showing the growth assembly. The 2-D growth system, showing the growth pouch on one side. (**A**) The growth paper was inserted within the cover sheet that has had the bottom end removed. A rubber band and binder hold two germination pouches firmly in place to the acrylic plate. (**B**) The germinated seed shows the RSA of the wheat seedling at the two-leaf stage. (**C**) An assembled 2-D growth system showing growth pouches hanging from a metal frame.

Statistical analysis of the results obtained from RootNav was processed and analyzed using IBM SPSS Statistics for Windows, v25.0 (IBM Corp., NY, USA). The results obtained were expressed as mean values for each parental line for each trait. Analysis of variance (ANOVA) was applied to compare the means. Based on the outcome of the ANOVA on all data, Tukey HSD post hoc analysis was performed to separate the means.

Spearman rank correlation coefficients (ϱ) was used to determine associations between measured traits. Data analysis and visualization of the mixed model was performed using R software Version 3.4.3.

3. Results

The root of the wheat seedlings grew freely along the airspace between the clear propylene sheet and the moistened blue absorbent growth paper without growing into the paper. This allowed for the capturing of clearly distinguishable root images from the blue germination paper. RootNav software (1.8.1) was used to extract the quantification of RSA traits from the total root images of 312 seedlings that were captured 7 days after planting.

3.1. Frequency Distribution of Germination Potential and Measured Root Traits

The germination potential of each accessions is shown in Figure 5. The average germination rate of hexaploid was 9.4% higher than the tetraploid wheat accessions. The frequency distribution of the germination potential showed that 85.3% of all accessions exceeded a 90% germination rate (Supplementary Figure S1).
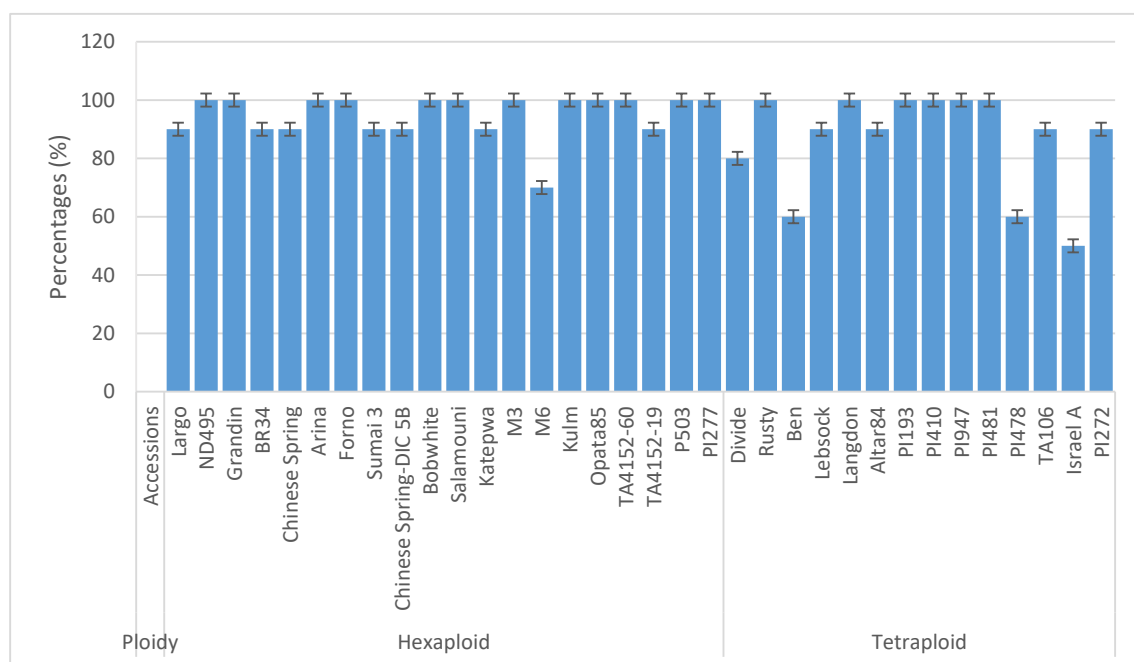

Figure 5. Germination potential for each accession.

The frequency histograms of the measured root traits for the 34 accessions are shown in Supplementary Figure S2. There was a strong correlation (0.8) between observed traits of total seminal root length and convex hull area. The average seminal length was strongly correlated (0.8) with maximum depth and centroid, while maximum width highly correlated (0.9) with width–depth ratio and convex hull area. The maximum depth also showed a high correlation (0.9) with a centroid (Figure 6).
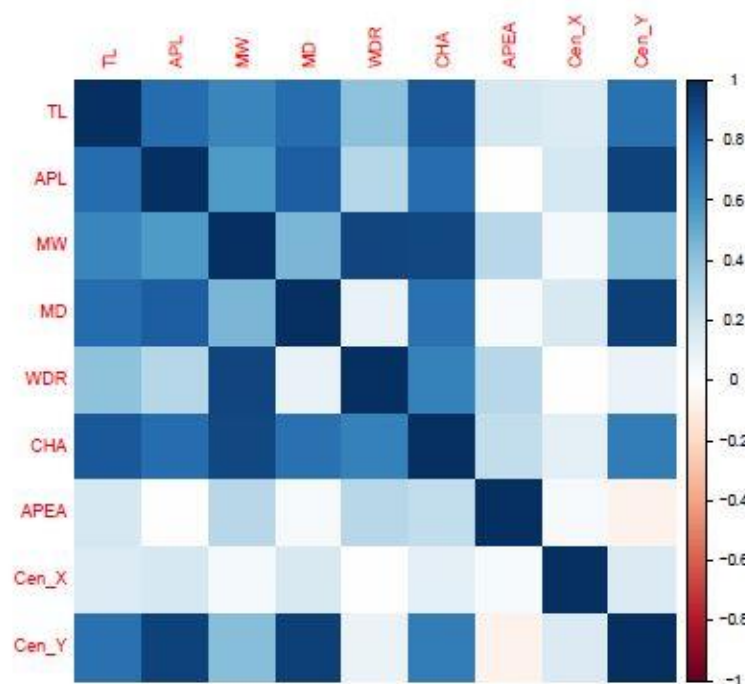
Figure 6. Correlation matrix of the measured root traits.

3.2. The Hexaploid Wheat Accessions

The non-destructive measurements of the RSA roots in Table 2 showed that the mean total length of Salamouni, Katepwa, Kulm, Opata85, TA60, Grandin, P503, Arina, Forno, Sumai3, and Chinese Spring-DIC 5B were significantly longer compared with Largo, which was used as the reference, by 0.9, 1.3, 1.9, 2.1, 1.5, 1.6, 0.9, 1.3, and 1.4 times, respectively. The average seminal length of Kulm, Opata85, TA60, Grandin, P503, Arina, and Forno compared to Largo were significantly longer, by 1.0, 1.0, 1.2, 0.8 1.0, 1.0, and 1.2 times, respectively. The mean count of the seminal root of Katepwa, Kulm, Opata85, and Grandin was significantly higher compared with Largo, by 0.5, 0.4, 0.5 and 0.4, times respectively. The mean maximum width showed that Kulm, Opata85, and Grandin were significantly larger compared with Largo, by 2.2, 1.4 and 1.7 times, respectively. The maximum depth of Kulm, Opata85, TA60, Grandin, P503, Arina, Forno, Sumai3, and Chinese Spring-DIC 5B were significantly greater compared with Largo, by 0.7, 0.8, 0.8, 0.6, 0.7, 0.7, 1.0, 0.8, and 0.8 times, respectively. The width to depth ratio of Kulm was significantly larger compared with Largo, by 0.9 times. The mean convex hull area of Kulm, Opata85, TA60, Grandin, and Arina were significantly larger compared to Largo, by 5.3, 4.8, 3.3, 4.1 and 3.1 times, respectively. The vertical coordinate of the centroid showed that Kulm, Opata85, TA60, TA19, P503, Arina, Forno, Sumai3, and Chinese Spring-DIC 5B were significantly greater compared with Largo, by 0.8, 1.0, 1.2, 0.8, 1.0, 1.1, 1.5, 1.0, 0.9 times, respectively.

Table 2. Root system architecture traits measured in 19 wheat accessions (hexaploid). The bolded mean values showed level of significance at $p < 0.05$ compared to the reference accession (Largo). Each trait has a column representing the mean value of 10 replicates for each accession followed by their standard deviation.

Accession	Total Length Mean	STD	Seminal Length Mean	STD	Seminal Count Mean	STD	Maximum Width Mean	STD	Maximum Depth Mean	STD	Width-Depth Ratio Mean	STD	Convex Hull Area Mean	STD	Seminal Emergence Angle Mean	STD	Centroid_X Mean	STD	Centroid_Y Mean	STD
Largo	1407.054	444.8384	400.8567	127.1285	3.56	0.726	332.22	179.31	751.89	182	0.4569	0.26354	105875	66594.71	22.6833	7.0495	−0.008	67.68921	193.0758	63.93469
ND495	1991.549	383.8933	532.204	207.123	4	0.816	378.8	260.032	1017.9	187.838	0.3512	0.19509	188694.2	162351.9	29.39	9.58095	3.6871	43.52455	279.4124	100.8176
Salamouni	**2628.581**	1295.576	611.519	269.4623	4.1	1.449	416.2	256.94	944.5	319.004	0.4251	0.24228	226789.1	154967.4	23.224	27.50345	76.3194	87.27794	277.9139	125.8842
Katepwa	**3251.233**	668.9902	644.2344	221.368	**5.22**	0.833	572.44	285.073	1035.33	210.224	0.5466	0.23586	333568.1	213121.5	31.5122	15.02541	9.21678	111.8648	278.9432	89.18816
M3	2051.728	955.6283	531.802	145.6446	3.7	1.059	224.3	148.072	989.8	271.476	0.2196	0.12853	126481.6	117850.5	19.818	13.55339	−4.9703	51.40844	284.2637	93.55736
M6	1701.343	876.2018	504.2471	196.2748	3.29	1.254	278.57	178.362	860.29	241.249	0.3064	0.19161	120445.6	85442.86	23.2343	23.46807	26.79043	50.84016	239.2451	95.57134
Kulm	**4071.759**	780.7794	**800.521**	166.8296	**5**	0.471	**1075**	240.575	**1274.8**	297.392	**0.8693**	0.21052	**671934.4**	282573.1	30.945	3.86432	34.0647	110.5345	**354.779**	87.14734
Opata	**4372.535**	947.7119	**786.908**	224.1664	**5.3**	0.675	803.7	329.924	**1355.4**	202.447	0.595	0.2199	**611183.9**	348976.6	23.772	6.56108	0.5184	83.79973	**383.1734**	75.31793
TA60	**3453.33**	739.9634	**872.307**	305.9635	4.1	0.876	632.8	283.294	**1351.1**	293.192	0.4748	0.20016	**451817.1**	236567.4	19.944	7.12346	43.7792	88.52216	**433.4055**	133.3076
TA19	2331.48	441.3384	680.5678	183.436	3.56	0.726	221.22	186.238	1052.78	147.466	0.2186	0.21618	116801.6	74324.72	20.8933	6.69294	1.45578	49.8508	356.9752	70.49687
Grandin	**3649.392**	689.1213	**727.775**	157.4818	**5.1**	0.738	**902.9**	368.004	**1177.09**	294.013	0.803	0.41375	**536945.6**	253719	39.773	12.66347	9.7508	60.9755	334.9114	75.75706
P503	**2635.32**	451.2482	815.313	167.5469	3.3	0.675	567.6	341.986	**1288.2**	244.35	0.4742	0.33644	336351.3	164600.2	35.085	18.39818	28.2041	62.06401	**390.4914**	94.16569
BR34	2486.309	621.315	625.36	193.1676	4	0.866	505.11	162.079	1114.33	325.571	0.4858	0.17914	277661.6	117046.7	25.4289	7.82762	44.02322	37.9747	322.6331	110.6642
CSpring	2526.974	787.4891	599.1433	226.2535	4.33	1.225	366.78	197.488	1106.89	265.426	0.3302	0.16149	212942.8	131228.1	35.7667	6.43028	1.78556	73.44133	297.4512	127.6352
Arina	**3211.019**	799.5607	818.916	197.3953	4	0.816	623.2	283.085	**1307.3**	213.307	0.491	0.23865	**430168.5**	185150.7	24.287	10.61435	70.9476	114.6787	**403.6996**	86.95764
Forno	**2856.862**	514.3885	**891.16**	116.4221	3.2	0.422	302.1	170.187	**1499.6**	281.496	0.2054	0.10853	246348	136554.2	24.115	15.79232	62.0981	91.38127	**489.6822**	94.50695
Sumai3	**3292.031**	700.3864	700.5822	186.8713	4.78	0.667	332.11	130.143	**1330.11**	191.472	0.2538	0.10798	252744.3	128540.6	19.75	10.36522	8.46689	64.34472	**394.5089**	85.76959
CSpringDIC	**3409.904**	589.5194	704.0922	127.4161	4.89	0.601	532.78	243.404	**1327.78**	172.431	0.3948	0.16589	401419.2	188296.1	23.9867	10.9366	26.17744	51.21258	**373.2856**	67.95206
Bobwhite	2354.442	708.3413	723.972	213.3244	3.3	0.675	452	333.689	1155.6	244.926	0.3768	0.26688	248701.9	195832.2	17.424	7.47542	33.4653	65.00261	346.2481	85.93454

3.3. The Tetraploid Wheat Accessions

Accessions Langdon, PI 193883, PI 41025, PI 94749, and PI 272 were significantly higher in mean total length compared with Rusty (which was used as a reference) by 1.4, 1.6, 1.6, 1.8, and 1.4 times, respectively as shown in Table 3. For mean seminal length, Lebsock, PI 193883, PI 41025, and PI 94749 showed a significantly longer seminal root, with 1.5, 1.4, 1.6, and 1.5 times more than Rusty.

For the mean maximum width, PI 277 showed a significant difference, increasing 1.7 times more than Rusty. For mean maximum depth, PI 193, PI 410 and PI272 showed a significant difference, increasing 0.9, 0.8, and 0.8 times more than Rusty, respectively. For the mean width to depth ratio, the PI 277 showed a significant increase of 1.1 times more than Rusty (Table 3).

In other measured root trait, the mean convex hull area of PI 193883 significantly increased by 3.1 times when compared to Rusty. For centroid_Y, Lebsock, PI 193, PI 410 and Israel showed a significant difference, increasing 1.4, 1.6, 1.5 and 1.6 times respectively.

Table 3. Root system architecture traits measured in 15 wheat accessions (tetraploid). The bolded mean values showed level of significance at $p < 0.05$ compared to the reference accession (Rusty). Each trait has a column representing the mean value of 10 replicates for each accession followed by their standard deviation.

Accession	Total Length Mean	STD	Seminal Length Mean	STD	Seminal Count Mean	STD	Maximum Width Mean	STD	Maximum Depth Mean	STD	Width-Depth Ratio Mean	STD	Convex Hull Area Mean	STD	Seminal Emergence Angle Mean	STD	Centroid_X Mean	STD	Centroid_Y Mean	STD
Divide	2451.268	1990.837	556.8063	377.8616	3.75	1.909	179.5	183.808	968	467.962	0.163	0.11099	132953.1	141900.5	24.745	11.29471	62.338	54.1888	285.8023	183.9844
Rusty	1390.807	1255.677	314.033	226.8649	3.9	1.101	289.9	323.018	668.2	296.794	0.355	0.30589	117461.6	178758.6	19.006	10.84459	1.5814	46.94676	148.5815	108.4252
Ben	3226.34	1606.199	613.275	250.9193	4.67	1.862	325.5	176.039	1041.17	364.806	0.2894	0.17678	192996.1	100061.9	17.0567	6.29637	−7.84817	31.76269	322.1412	136.3388
Lebsock	2709.894	1156.688	**782.76**	384.2838	3.56	1.13	352.78	215.12	1064.44	330.105	0.3325	0.18338	234695.5	203638.2	12.5878	12.2572	82.69922	67.46444	**361.4402**	171.0809
Langdon	**3344.535**	910.3358	647.958	140.2428	5.1	0.568	541.6	228.824	1119.8	198.192	0.4879	0.19377	319992.9	119248.3	31.939	15.33947	−9.1897	60.98329	328.3687	72.69708
Altar	2509.834	1114.787	529.8867	216.3208	4.78	1.202	559.33	327.655	951.56	284.677	0.5769	0.27336	261532.6	218210.9	25.2367	12.27078	3.87411	44.27495	230.5439	106.7623
PI193	**3673.169**	1406.628	**745.731**	256.8887	4.9	0.738	589.9	298.531	**1266**	337.197	0.4442	0.17098	**484674.4**	318533.1	25.628	12.4758	−71.1325	67.57832	**385.4912**	132.6479
PI410	**3583.227**	1531.398	**814.01**	338.0744	4.5	1.08	494.5	248.758	**1211.7**	369.315	0.4068	0.14769	351557.5	262529.1	15.345	6.84556	95.9932	142.1959	**373.7213**	141.8784
PI947	**3931.771**	1070.18	**772.071**	210.8183	5.1	0.568	647.8	167.364	1125.7	280.126	0.6101	0.23353	389343.7	188785.1	34.931	8.18785	54.9579	125.2904	334.0316	96.79933
PI481	1971.452	905.4402	707.311	291.7558	2.8	0.422	283.2	176.585	1045.6	315.264	0.2587	0.1009	162980	161573.2	17.845	13.14568	−1.4536	44.00917	340.9898	134.9614
PI478	1060.158	414.0258	449.97	99.81476	2.33	0.816	230	138.466	801.83	138.077	0.2761	0.16724	75115.56	49265.76	15.71	9.12903	−1.32917	29.95209	214.8288	41.66894
TA106	1789.02	682.8475	596.3411	227.6161	3	0	515	274.868	944.22	258.074	0.5188	0.18626	226387.3	185876.3	17.5533	7.23385	−3.023	18.78727	275.3341	94.02308
Israel	2400.58	1152.096	814.988	352.7714	2.8	0.447	552.8	345.331	1215.6	395.11	0.4045	0.19579	331445.6	247329.2	18.316	9.29823	7.3922	39.28395	**391.6284**	161.1772
PI277	2494.331	756.1297	586.835	250.0628	4.4	0.699	**769.1**	268.301	1056.8	313.966	**0.7469**	0.24797	388875.3	231645.1	27.434	9.31469	52.6313	47.89209	289.165	126.5571
PI272	**3406.442**	1182.352	726.5822	217.0046	4.67	0.707	623	258.412	**1232.33**	278.285	0.5107	0.18407	418640.8	225100.3	26.1411	12.37334	62.85044	61.72506	342.3118	119.2106

4. Discussion

The root phenotyping pipeline, examined in this study using a germination paper-based moisture replacement system, allowed the measurement of important root architectural traits to be collected in an efficient, low-cost, and high-throughput fashion.

4.1. The Benefit of the Root System Size

The root system size is the representation of the total root length, seminal count, and the convex hull area. In previous studies, these traits have been positively associated with each other as well as with the grain yield of wheat in the field [22,23]. We also found a significant correlation between the total root length, maximum depth and the convex hull area in this study. A higher total root length does not always signify a deeper root growth, as the total length of seminal roots is the result of many seminal roots. Therefore, the addition of another pair of seminal roots to the root system results in a longer seminal root length as well, but not automatically in a deeper root system. Therefore, this results in an average seminal root length (defined as the total seminal length divided by the seminal root count), a preferable trait to allow root growth than total length, as a deeper root system may help to access deep water and mobile nutrients. In addition, the average seminal root length trait showed a significant correlation with both total root length and the convex hull area, which agrees with previous findings [32] that suggested that deeper penetration of the soil by seedling roots may result in better access to mobile soil nutrients and early plant establishment. The total root length and the average seminal root length had strong associations with the centroid_Y (vertical axis), which is suggested to be responsible for the aboveground vigor and root depth of the plant [12]. Based on our study, the use of average seminal length traits to assess variations in the RSA of wheat seedling is recommended because of its ability to delineate the performance of most of the wheat accessions, and at the same time showing a strong correlation with the next three important traits: total length, maximum depth and convex hull area.

4.2. Kulm and Opata85 May be Useful for RSA Improvement in Hexaploid Wheat

Kulm is a hard-red spring wheat (HRSW) developed at North Dakota State University, Fargo, ND. In our study, Kulm performed better than all the other accessions we examined under the same environmental conditions. Kulm had a higher mean total length, mean average primary length, seminal count and convex hull area, making it a suitable candidate for breeding a larger root system and greater spatial distribution. Kulm has been used in previous studies as a parental line for inbred line developments [33,34] with a report affirming its higher yield. Although Kulm has been found susceptible to some wheat pathogens, like septoria tritici blotch (STB) [34], *septoria nodorum* blotch (SNB) and tan spot [35], it remains a good candidate for the selection of grain-end-use quality [33].

Opata 85 is a commercial spring wheat cultivar developed at International Maize and Wheat Improvement Center (CIMMYT), Mexico [36]. In our study, the next best accession after Kulm was Opata85, as it produced more roots and an overall architecture that allowed it to occupy a greater root area. These traits make Opata 85 a suitable breeding candidate for larger root development and improvements in abiotic stress resistance. Opata 85 has been used as a parental line for recombinant inbred lines (RILs) used to map yield traits [37], important agronomic traits [36], growth characters [38], water-logging tolerance in seed germination and seedling growth [39], and growth duration components [40].

4.3. The Significance of a Rapid Screening Pipeline for Measuring Seedling Root Traits

The high-throughput root phenotyping pipeline that was developed in this study revealed variation in seedling root traits of both hexaploid and tetraploid wheat accessions. The pipeline allowed us to examine the root system architecture of 340 wheat seedlings, using only one out of four sections of our metal scaffoldings, that were fitted with three solution tanks. Each section has the

capacity to fit 84 growth systems that allow the screening of approximately 168 seedlings for each assembly. The total capacity of the platform can allow phenotypic evaluation of 672 plants per run in the fixed temperature growth room within 10 days, and this includes the assembling of a 2-D growth system and image analysis. Acquisition of root images of 168 seedlings takes approximately 3.5 hours, while the semi-automated image analysis using open source software takes 1.5mins per image. This is slightly more time efficient than the method of Atkinson et al., [12] who reported ~2mins per image and ~5 mins per plant.

The cost of the 2D-growth system is ~ \$0.43 per plant with a reusable acrylic sheet of ~ \$3.30. The overall growth system assembly for the first time will cost \$4.20 with a recurring cost of \$0.90 per system. This is 81% lower than the average available market price of seed germination pouches.

Although different phenotyping systems based on germination paper have been reported in previous studies [15,32,33], the pipeline described in this study is similar to the pouch and wick hydroponic-based system [12]. However, the pipeline in our study was enhanced by adding vapor sterilization of the seeds; positioning the wheat seeds at a strategic angle that improved root images; growing two (2) plants per growth system; and utilization of separable solution tanks that can hold up to 4L of nutrient solution and 28 growth systems. The advantage of this type of solution tank for further investigation is that root response to abiotic stress and different nutrient regimes [41] can be assessed by varying solution constituent. Recently, Shorinola et al. [42] implemented this phenotyping pipeline to conduct a forward genetic screening for variation analysis of seminal root in a Cadenza mutant population.

4.4. Future Work

SHW lines have become valuable resources for the genetic improvement of common wheat cultivars [29]. The findings of the variation analysis from this study will allow us to investigate segregating mapping populations that will include the RILs of M3 and Kulm; and M6 and Opata85. M3 was developed at CIMMYT, Mexico whereas Kulm was developed at North Dakota State University, Fargo, ND. These hexaploids are both spring type, with M3 being a synthetic hexaploid while Kulm is a hard-red spring wheat [34]. The associative mapping population that resulted from the crossing of these two lines (Kulm × M3) resulted in the 105 RILs that will be used in further studies of the hexaploid lines. Additionally, 114 RILs resulting from the hexaploid mapping population of Opata85 × M6 and chromosome substitution lines involving PI 478742, a tetraploid (where individual pairs of chromosomes of wild emmer have been substituted for homologous pairs of chromosomes in background of Langdon durum), will be evaluated to identify the chromosome locations of loci responsible for the differences in RSA traits. Thereafter, molecular markers suitable for the marker-assisted selection of these traits will be developed.

5. Conclusions

In this study, we have studied RSA on 34 different wheat accessions at an early stage of plant development and were able to demonstrate its use in identifying accessions which perform better than others in some of the RSA characters. This study clearly possesses an advantage over the previously reported study because of its capacity to increase screening potential at early stages of plant development. This pipeline is also very simple and provides an opportunity for automation of acquisition of the RSA images (Step 3 of Figure 2) and screening platforms. The availability of mapping populations and high-resolution mapping data from these accessions provides an opportunity for utilizing this pipeline in identifying QTLs linked to RSA in populations segregating in RSA traits.

Author Contributions: The method was conceived, designed, and coordinated by A.T. The experiment was performed by E.A., R.M. and W.M. The data were analyzed and results interpreted by E.A., E.A. wrote

Abbreviations

TL	Total length;
APL	Average seminal length;
MW	Maximum width;
MD	Maximum depth;
WDR	Width-depth ratio;
CHA	Convex hull area;
APEA	Average seminal emergence area;
Cen_X	Horizontal coordinates of centroid;
Cen_Y	Vertical coordinates of centroid;
PC	Seminal count.

References

1. Khan, M.A.; Gemenet, D.C.; Villordon, A. Root System Architecture and Abiotic Stress Tolerance: Current Knowledge in Root and Tuber Crops. *Front Plant Sci.* **2016**, *7*, 1584. [CrossRef] [PubMed]
2. Smith, S.; De Smet, I. Root system architecture: Insights from Arabidopsis and cereal crops. *Philos. Trans R. Soc. B Biol. Sci.* **2012**, *367*, 1441–1452. [CrossRef] [PubMed]
3. Meister, R.; Rajani, M.S.; Ruzicka, D.; Schachtman, D.P. Challenges of modifying root traits in crops for agriculture. *Trends Plant Sci.* **2014**, *19*, 779–788. [CrossRef] [PubMed]
4. Lynch, J.; French, A.P.; Atkinson, J.A.; Wells, D.M.; Bennett, M.; Pridmore, T. Root Architecture and Plant Productivity. *Plant Physiol.* **1995**, *109*, 7–13. [CrossRef] [PubMed]
5. de Dorlodot, S.; Forster, B.; Pagès, L.; Price, A.; Tuberosa, R.; Draye, X. Root system architecture: Opportunities and constraints for genetic improvement of crops. *Trends Plant Sci.* **2007**, *12*, 474–481. [CrossRef] [PubMed]
6. Shewry, P.R. Wheat. *J. Exp. Bot.* **2009**, *60*, 1537–1553. [CrossRef] [PubMed]
7. Mayer, K.X. A chromosome-based draft sequence of the hexaploid bread wheat (*Triticum aestivum*) genome. *Science* **2014**, *345*, 1251788.
8. Boyacioglu, H. Global Durum Wheat Use Trending Upward. Available online: https://www.world-grain. com/articles/8777-global-durum-wheat-use-trending-upward (accessed on 31 January 2020).
9. Weiss, E.; Zohary, D. The Neolithic Southwest Asian Founder Crops. *Curr. Anthropol.* **2011**, *52*, S237–S254. [CrossRef]
10. Shu, K.; Liu, X.; Xie, Q.; He, Z.; X-d, L. Two Faces of One Seed: Hormonal Regulation of Dormancy and Germination. *Mol. Plant* **2016**, *9*, 34–45. [CrossRef]
11. Ma, Z.; Bykova, N.V.; Igamberdiev, A.U. Cell signaling mechanisms and metabolic regulation of germination and dormancy in barley seeds. *Crop J.* **2017**, *5*, 459–477. [CrossRef]
12. Atkinson, J.A.; Wingen, L.U.; Griffiths, M.; Pound, M.P.; Gaju, O.; Foulkes, M.J.; Le Gouis, J.; Griffiths, S.; Bennett, M.J.; King, J.; et al. Phenotyping pipeline reveals major seedling root growth QTL in hexaploid wheat. *J. Exp. Bot.* **2015**, *66*, 2283–2292. [CrossRef] [PubMed]
13. Zadoks, J.C.; Chang, T.T.; Konzak, C.F. A decimal code for the growth stages of cereals. *Weed Res.* **1974**, *14*, 415–421. [CrossRef]
14. Fischer, R.A.; Edmeades, G.O. Breeding and Cereal Yield Progress. *Crop Sci.* **2010**, *50*, S85. [CrossRef]
15. Richard, C.; Hickey, L.T.; Fletcher, S.; Jennings, R.; Chenu, K.; Christopher, J.T. High-throughput phenotyping of seminal root traits in wheat. *Plant Methods* **2015**, *11*, 13. [CrossRef]
16. Schroth, G.; Kolbe, D. A method of processing soil core samples for root studies by subsampling. *Biol. Fertil. Soils* **1994**, *18*, 60–62. [CrossRef]

17. Trachsel, S.; Kaeppler, S.M.; Brown, K.M.; Lynch, J.P. Shovelomics: High throughput phenotyping of maize (*Zea mays* L.) root architecture in the field. *Plant Soil* **2011**, *341*, 75–87. [CrossRef]

18. Xie, Q.; Fernando, K.M.C.; Mayes, S.; Sparkes, D.L. Identifying seedling root architectural traits associated with yield and yield components in wheat. *Ann. Bot.* **2017**, *119*, 1115–1129. [CrossRef]

19. Liu, X.; Li, R.; Chang, X.; Jing, R. Mapping QTLs for seedling root traits in a doubled haploid wheat population under different water regimes. *Euphytica* **2013**, *189*, 51–66. [CrossRef]

20. Cobb, J.N.; DeClerck, G.; Greenberg, A.; Clark, R.; McCouch, S. Next-generation phenotyping: Requirements and strategies for enhancing our understanding of genotype-phenotype relationships and its relevance to crop improvement. *Theor. Appl. Genet.* **2013**, *126*, 867–887. [CrossRef]

21. Hund, A.; Trachsel, S.; Stamp, P. Growth of axile and lateral roots of maize: I development of a phenotying platform. *Plant Soil* **2009**, *325*, 335–349. [CrossRef]

22. Gioia, T.; Galinski, A.; Lenz, H.; Müller, C.; Lentz, J.; Heinz, K.; Briese, C.; Putz, A.; Fiorani, F.; Watt, M.; et al. GrowScreen-PaGe, a non-invasive, high-throughput phenotyping system based on germination paper to quantify crop phenotypic diversity and plasticity of root traits under varying nutrient supply. *Funct. Plant Biol.* **2017**, *44*, 76–93. [CrossRef]

23. Bonser, A.M.; Lynch, J.; Snapp, S. Effect of phosphorus deficiency on growth angle of basal roots in Phaseolus vulgaris. *New Phytol.* **1996**, *132*, 281–288. [CrossRef] [PubMed]

24. Dupuy, L.X.; Wright, G.; Thompson, J.A.; Taylor, A.; Dekeyser, S.; White, C.P.; Thomas, W.T.B.; Nightingale, M.; Hammond, J.P.; Graham, N.S.; et al. Accelerating root system phenotyping of seedlings through a computer-assisted processing pipeline. *Plant Methods* **2017**, *13*, 1–14. [CrossRef] [PubMed]

25. Chen, Y.L.; Dunbabin, V.M.; Diggle, A.J.; Siddique, K.H.M.; Rengel, Z. Development of a novel semi-hydroponic phenotyping system for studying root architecture. *Funct. Plant Biol.* **2011**, *38*, 355. [CrossRef]

26. Zhou, T.; Wang, L.; Li, S.; Gao, Y.; Du, Y.; Zhao, L.; Liu, W.; Yang, W. Interactions Between Light Intensity and Phosphorus Nutrition Affect the P Uptake Capacity of Maize and Soybean Seedling in a Low Light Intensity Area. *Front Plant Sci.* **2019**, *10*, 1–15. [CrossRef] [PubMed]

27. Joshi, D.C.; Singh, V.; Hunt, C.; Mace, E.; van Oosterom, E.; Sulman, R.; Jordan, D.; Hammer, G. Development of a phenotyping platform for high throughput screening of nodal root angle in sorghum. *Plant Methods* **2017**, *13*, 56. [CrossRef]

28. Pound, M.P.; French, A.P.; Atkinson, J.A.; Wells, D.M.; Bennett, M.J.; Pridmore, T. RootNav: Navigating images of complex root architectures. *Plant Physiol.* **2013**, *162*, 1802–1814. [CrossRef]

29. Li, A.; Liu, D.; Yang, W.; Kishii, M.; Mao, L. Synthetic Hexaploid Wheat: Yesterday, Today, and Tomorrow. *Engineering* **2018**, *4*, 552–558. [CrossRef]

30. Clough, S.J.; Bent, A.F. Floral dip: A simplified method for Agrobacterium-mediated transformation of Arabidopsis thaliana. *Plant J.* **1998**, *16*, 735–743. [CrossRef]

31. Hoagland, D.R.; Arnon, D.I. The Water-Culture Method for Growing Plants without Soil. *Circ. Calif. Agric. Exp. Stn.* **1950**, *347*, 32.

32. Cao, P.; Ren, Y.; Zhang, K.; Teng, W.; Zhao, X.; Dong, Z.; Liu, X.; Qin, H.; Li, Z.; Wang, D.; et al. Further genetic analysis of a major quantitative trait locus controlling root length and related traits in common wheat. *Mol. Breed.* **2014**, *33*, 975–985. [CrossRef]

33. Mergoum, M.; Frohberg, R.C.; Rasmussen, J.W.; Friesen, T.L.; Hareland, G.; Simsek, S. Breeding for CLEARFIELD Herbicide Tolerance: Registration of 'ND901CL' Spring Wheat. *J. Plant Regist.* **2009**, *3*, 170–174. [CrossRef]

34. Ghaffary, S.M.T.; Faris, J.D.; Friesen, T.L.; Visser, R.G.F.; van der Lee, T.A.J.; Robert, O.; Kema, G.H.J. New broad-spectrum resistance to septoria tritici blotch derived from synthetic hexaploid wheat. *Theor. Appl. Genet.* **2012**, *124*, 125–142. [CrossRef] [PubMed]

35. Faris, J.D.; Zhang, Z.; Lu, H.; Lu, S.; Reddy, L.; Cloutier, S.; Fellers, J.P.; Meinhardt, S.W.; Rasmussen, J.B.; Xu, S.S.; et al. A unique wheat disease resistance-like gene governs effector-triggered susceptibility to necrotrophic pathogens. *Proc. Natl. Acad. Sci. USA* **2010**, *107*, 13544–13549. [CrossRef]

36. Borner, A.; Schumann, E.; Furste, A.; Coster, H.; Leithold, B.; Roder, M.; Weber, W. Mapping of quantitative trait loci determining agronomic important characters in hexaploid wheat (*Triticum aestivum* L.). *Theor. Appl. Genet.* **2002**, *105*, 921–936. [CrossRef]

37. Kumar, N.; Kulwal, P.L.; Balyan, H.S.; Gupta, P.K. QTL mapping for yield and yield contributing traits in two mapping populations of bread wheat. *Mol. Breed.* **2007**, *19*, 163–177. [CrossRef]

38. Kulwal, P.; Roy, J.; Balyan, H.; Gupta, P. QTL mapping for growth and leaf characters in bread wheat. *Plant Sci.* **2003**, *164*, 267–277. [CrossRef]

39. Yu, M.; Mao, S.; Chen, G.; Liu, Y.; Li, W.; Wei, Y.; Liu, C.; Zheng, Y. QTLs for Waterlogging Tolerance at Germination and Seedling Stages in Population of Recombinant Inbred Lines Derived from a Cross Between Synthetic and Cultivated Wheat Genotypes. *J. Integr. Agric.* **2014**, *13*, 31–39. [CrossRef]

40. Yu, M.; Chen, G.-Y.; Pu, Z.-E.; Zhang, L.-Q.; Liu, D.-C.; Lan, X.-J.; Wei, Y.-M.; Zheng, Y.-L. Quantitative trait locus mapping for growth duration and its timing components in wheat. *Mol. Breed.* **2015**, *35*, 44. [CrossRef]

41. Ingram, P.A.; Zhu, J.; Shariff, A.; Davis, I.W.; Benfey, P.N.; Elich, T. High-throughput imaging and analysis of root system architecture in Brachypodium distachyon under differential nutrient availability. *Philos. Trans. R. Soc. Lond. B Biol. Sci.* **2012**, *367*, 1559–1569. [CrossRef]

42. Shorinola, O.; Kaye, R.; Golan, G.; Peleg, Z.; Kepinski, S.; Uauy, C. Genetic screening for mutants with altered seminal root numbers in hexaploid wheat using a high-throughput root phenotyping platform. *G3* **2019**, *9*, 2799–2809. [CrossRef]